

Semiconductor A_3B_5 nanostructures for infrared femtosecond lasers

N N Rubtsova¹, S A Kochubei¹, A A Kovalyov¹,
V V Preobrazhenskii¹, M A Putyato¹, B R Semyagin¹,
T S Shamirzaev¹, G M Borisov¹, V E Kisel², N V Kuleshov²,
S V Kuril'chik², O V Buganov³, S A Tikhomirov³

¹A.V. Rzhanov Institute of Semiconductor Physics of Siberian Branch of Russian Academy of Sciences, 13, academician Lavrentyev prospect, Novosibirsk, 630090, Russia

²Scientific Research Institute for Optical Materials and Technologies of Belarus National Technical University, 65, Nezavisimosti avenue, bd. 17, 220013, Minsk, Belarus

³B.I. Stepanov Institute of Physics, National Academy of Sciences of Belarus, 68, Nezavisimosti avenue, Minsk, 220072, Belarus

E-mail: rubtsova@isp.nsc.ru

Abstract. Two techniques were suggested and tested for the recovery time shortening of saturable absorbers on a base of A_3B_5 compounds including quantum wells. The first one, proposed by authors, is the sample post-growth treatment by UV laser radiation; it implied generation of point defects, which, in its turn, led to electron-hole recombination acceleration and to recovery time shortening by an order of magnitude and more. Another technique based on special design of barriers gave promising results for the fast saturable absorbers. Semiconductor mirrors designed for $Yb^{3+}:KY(WO_4)_2$ infrared laser mode locking led to 115 fs stable mode-locking regime with average power close to CW operation. Results on fast saturable absorbers for spectral region of 1500 nm are also presented.

1. Introduction

The most suitable way to get the self-mode-locking in compact low-gain lasers is to use the saturable absorber (SA) [1]. The common used design of SA is based on thin layers of semiconductors including the quantum wells (QW) separated by barriers of another semiconductor. Three- or even four- component semiconductor alloys (ternary or quaternary) are the appropriate choice for a wide spectral region. In particular, A_3B_5 ternary and quaternary semiconductor compounds are well suited for short-pulse lasers operating in the spectral region of 1-3 microns [2]. SA including A_3B_5 quantum wells separated by thick barrier show electron-hole recombination rate of about hundreds of picoseconds [3].

Since many applications of ultra-short pulse lasers require high repetition rate of pulses, SA used for laser mode-locking have to meet this requirement. Several approaches to SA recovery time shortening by special technologies of molecular beam epitaxy (MBE) growth are known. Doping of QW layers by Be ions during MBE growth [4] shortened charge carrier recombination time to 0.25 ps. Application of sub-band gap states in semiconductor nitrides [5] resulted in relaxation rate of 12 ps. Intentional lattice mismatching by using metamorphic growth of InGaP on GaAs led to recovery time of 5 ps [6].

Another approach is based on SA post-growth processing. So, the post-growth irradiation of the sample by Ni^+ ions beam [7] resulted in relaxation rate of 2.4 ps.

The goal of this work is to analyze new approaches to SA recovery time shortening which could guarantee minimal losses of optical quality and persistence of excitonic contribution to absorption.

2. UV post-growth treatment

Our first results on UV post-growth treatment were obtained for SA operating in the near-infrared region [8]. In [8] definite doses of laser UV radiation could accelerate electron-hole recombination by 20 times. Here, we applied UV post-growth irradiation to SA designed for visible light in the vicinity of titanium-sapphire laser operation spectral region.

The sample was grown by MBE technique at the substrate of semi-insulating GaAs with (001) orientation. The rate of growth and layers thickness was controlled by reflective high energy electrons diffraction (RHEED) technique, and the crystal quality of the sample was controlled by X-ray diffraction. The sample consisted of 20 quantum wells of 3 nm thickness GaAs separated by 6 nm $\text{Al}_{0.38}\text{Ga}_{0.62}\text{As}$ barriers.

Pump-probe technique was applied to test the sample reflectivity kinetics. The femtosecond spectrometer operating in the spectral region of 760 - 820 nm provided 150 fs pulses of 1 mJ energy at repetition rate of 10 Hz. The pulsed output radiation at the central wavelength of 780 nm was divided into couple of beams. The most intense beam served as the pump beam. After the passage through the optical delay line, it was directed to the sample at the incidence close to the normal one, and it was focused into the spot of approximately 1 mm diameter. Another part, four times less intense, was used for the super-continuum generation in the cavity filled by water. The super-continuum radiation was divided in two beams — the reference one and the probe one. The reference beam meets the sample before the pump beam arrival. The probe beam arrived after the pump providing just the measured signal. The spectra of both reference and probe pulses reflected from the sample surface were detected by system including polychromator, CCD camera and microprocessor.

The change in the sample reflectivity $\log(R_0/R)$ (here R_0 is the sample reflectivity before pumping, R — after it) was determined as the function of time delay τ_{del} between the probe and the pump, and as the function of the probe radiation wavelength.

The result of UV irradiation was checked via reflectivity kinetics at the wavelength of 750 nm which corresponded to the sample photoluminescence band center.

Excimer XeCl laser operating at the radiation wavelength of 308 nm with pulse duration of 5 ns and repetition rate of 1 Hz was applied for the sample UV treatment. Result of UV radiation action was controlled through photoluminescence (PL) intensity change by registration of PL intensity before and after UV irradiation. In order to find how the irradiation conditions influence the final result, both the energy density of each UV pulse and the number of pulses influenced the sample were changing from one to another area of the sample. Since the energy of UV radiation quantum $E=4.03$ eV is comparable to the bonding energy of GaAs, we could expect the photochemical modification of the sample surface even at low UV radiation energy density. All the experiments were carried out at room temperature in the atmospheric air ambient.

Excimer laser UV radiation focusing into the spot of approximately 1 micron in diameter led to the laser plume formation over the sample surface. The spectrum of laser plume radiation was controlled by special set up including monochromator and registration system (photomultiplier, peak voltmeter, ADC and personal computer).

Fig. 1 shows sample PL spectra before (bold curve) and after (thin) UV irradiation for different energy densities; the left graphs correspond to 80 mJ/cm^2 , and the right one to 350 mJ/cm^2 . All the spectra demonstrate PL band centered at 1.66 eV and width at half maximum of about 30 meV. UV irradiation does not change PL spectral shape, but results in PL intensity

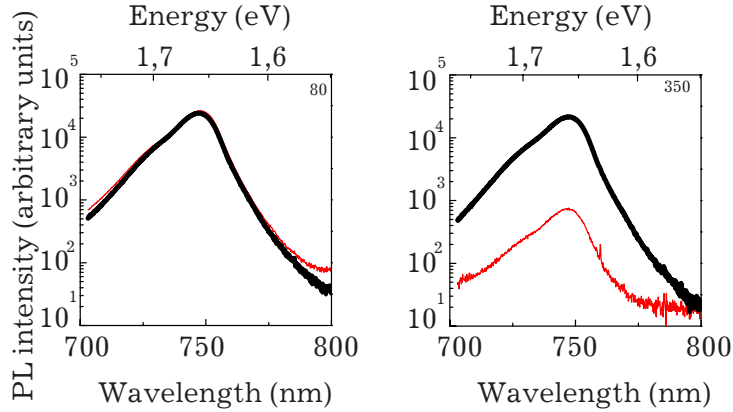


Figure 1. PL spectra of samples before (bold curve) and after (the thin one) UV irradiation for energy density of 80 mJ/cm^2 (left) and 350 mJ/cm^2 (right).

changes. These changes are minimal for UV energy density of 80 mJ/cm^2 , as it can be seen in the left graph of Fig. 1; PL intensity increase after irradiation seen at this graph should be attributed to the sample lateral inhomogeneity. Meanwhile, UV irradiation at energy density of 350 mJ/cm^2 results in remarkable (almost two orders of magnitude) decrease of PL intensity.

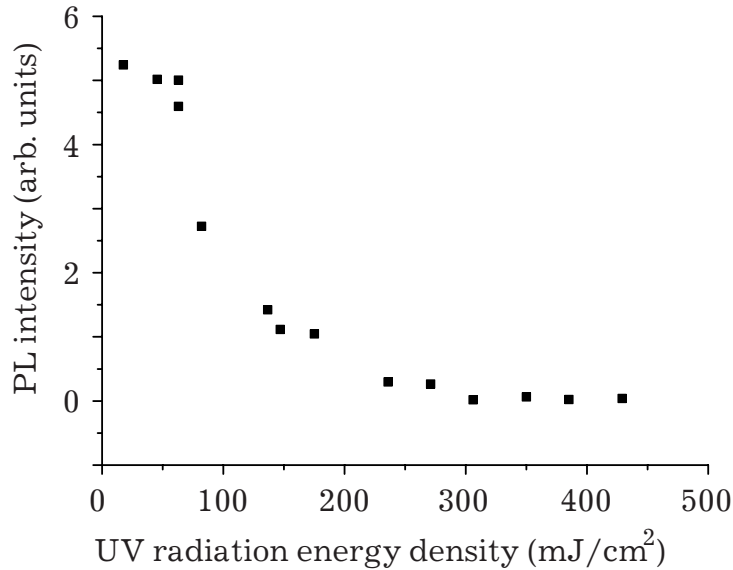


Figure 2. PL intensity of the sample as a function of UV energy density.

PL intensity (at the band center) of the sample treated by 5 UV pulses is shown in Fig. 2 versus UV energy density. PL intensity in the Fig. 2 was corrected to the above mentioned lateral inhomogeneity. As it can be seen from Fig. 2, there are no considerable PL intensity changes for UV energy density less than 100 mJ/cm^2 . At UV energy densities higher than 100 mJ/cm^2 , the fast decrease of PL intensity was observed. Such behaviour proves the threshold character of the phenomenon. Our results agree with [9] for laser induced point defects generation in bulk GaAs.

PL intensity change due to UV irradiation depends on the number of UV pulses too. This dependence is different for UV energy density under or above the threshold, as it can be seen

in Fig. 3. The sample PL intensity practically does not depend on number of UV pulses for low energy density (squares in Fig. 3). For UV energy density over threshold, the PL decreases as number of pulses grows (circles in Fig. 3).

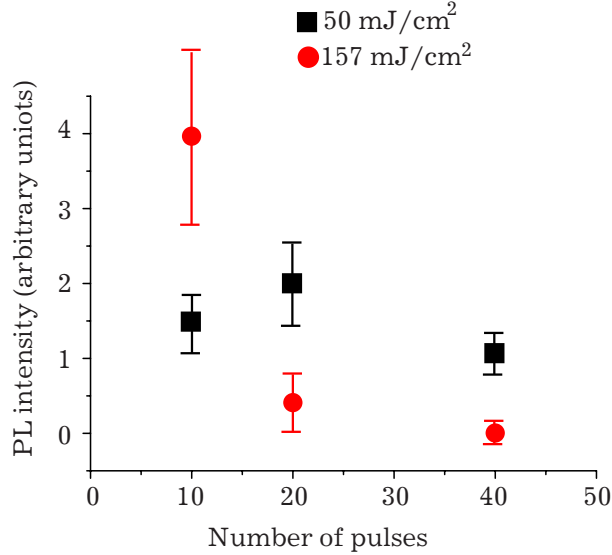


Figure 3. PL intensity dependence on the number of UV pulses may be weak (squares) or quite pronounced (circles) depending on the UV energy being below threshold or over it.

The most important effect of UV irradiation should be seen in the sample reflectivity kinetics. Really, Fig. 4 demonstrates how changes $\log(R_0/R)(\tau_{del}$ kinetics with UV energy density. Results in Fig. 4 were obtained for sample area irradiated by 5 UV pulses with different energy density — from top to bottom correspondingly 17.5 mJ/cm², 45.5 mJ/cm², and 100 mJ/cm². Squares with error bars represent experimental curves, the circles correspond to the model curves. Probe beam wavelength was chosen at PL band maximum (750 nm) for all kinetic curves in Fig. 4.

Evidently, relaxation rates grow as UV energy density increases, and some PL intensity decrease takes place too.

Specificity of a given SA sample is following. The band gap of GaAs at room temperature is 1.424 eV, which corresponds to the absorption edge near the wavelength of 870 nm. Quantum wells transition occurs at the energy 1.65 eV (wavelength 750 nm). The sample was excited by femtosecond pump radiation centered at 780 nm which corresponds to the light quantum energy 1.59 eV. Hence, both sample substrate GaAs and quantum well layers could absorb the pump pulse radiation — not only because of large femtosecond pulse spectral width, but also due to two-photon absorption.

That is why the model of relaxation kinetics accounted for the next processes: 1) excitons formation in quantum wells and increase of non-equilibrium quasi-two-dimensional charge carrier density — which induces fast increase of non-equilibrium reflectivity; 2) decrease of non-equilibrium charge carrier density because of non-radiative recombination due to interaction with defects — which implies non-equilibrium reflectivity relaxation; 3) absorption in the substrate GaAs and increase of non-equilibrium charge carrier density — which increases non-equilibrium reflectivity too; 4) electrons and holes recombination — which should result in reflectivity relaxation to its equilibrium value. The last process is usually the most slow, and it is the process which limits SA recovery time.

The formula accounting for all four above mentioned processes looks as:

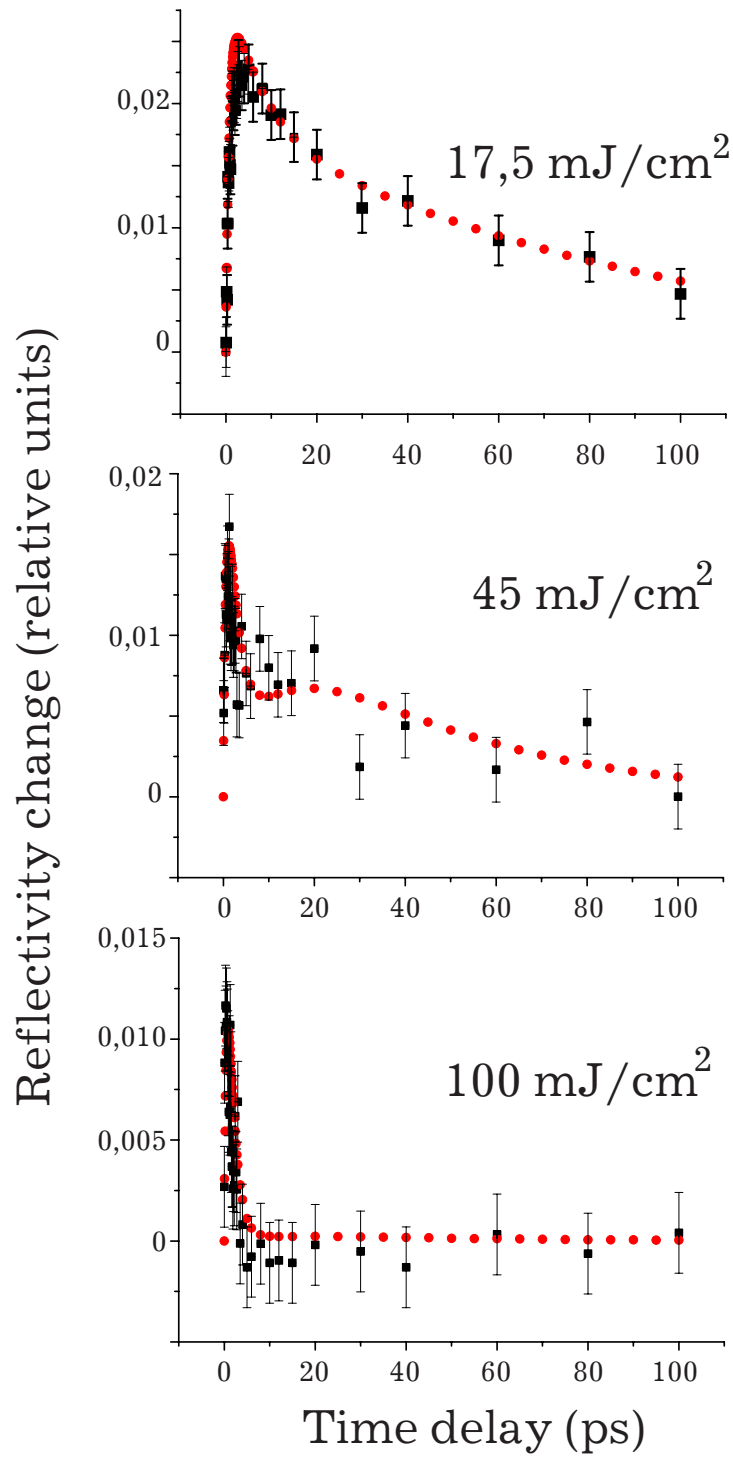


Figure 4. Reflectivity kinetics for the sample area irradiated by UV pulses of different energy density (indicated for each curve).

$$S(t) = a \cdot (1 - \exp(-t/\tau_1)) \cdot \exp(-t/\tau_2) + b \cdot (1 - \exp(-t/\tau_3)) \cdot \exp(-t/\tau_4) \quad (1)$$

Here τ_i are relaxation times of above mentioned processes; the constants a and b reflect relative contribution of quantum wells and of substrate into reflectivity change. The parameters a , b and τ_i were chosen in the course of mean square root fitting of experimental points by the model curves.

Table 1

UV energy density (mJ/cm ²)	17.7	45.5	100
τ_1 (ps)	0.8	0.8	0.8
τ_2 (ps)	10	2.5	1.5
τ_3 (ps)	15	15	15
τ_4 (ps)	80	40	40
a	0.03	0.03	0.03
b	0.02	0.015	0.0015

Table 1 shows relaxation times τ_i and amplitudes a and b for above mentioned processes fitted for three areas of the sample processed by UV radiation of energy density indicated in the first line of the table. The parameters b , τ_2 and τ_4 experience the most remarkable changes. From the viewpoint of general recovery of SA, the relaxation time τ_4 seems to be the most important. The acceleration of electron-hole recombination is also clearly seen from experimental and model curves in Fig. 4.

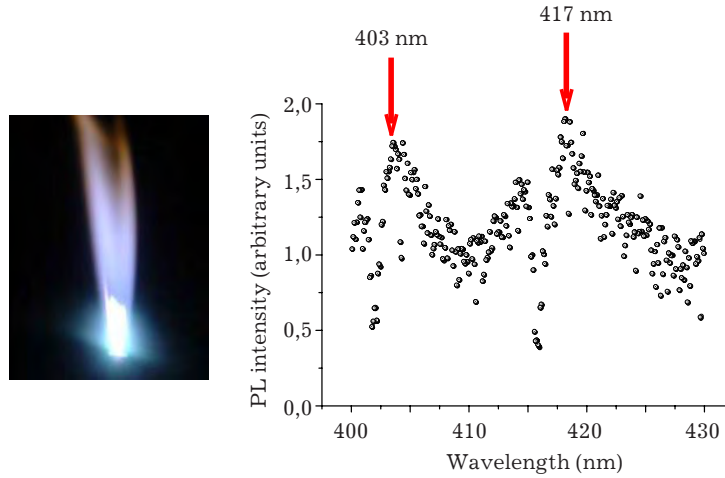


Figure 5. Laser plume over sample surface (left) and its emission spectrum (right).

Fig. 5 shows the laser plume generated over the sample surface as a result of UV focusing into the spot of 1 micron diameter (left) and its emission spectrum (right). Two peaks in laser plume emission spectra centered at wavelength 403 nm and 417 nm should be attributed to radiation of neutral Ga atoms and correspond to transitions ${}^2P^0_{1/2} - {}^2S^0_{1/2}$ and ${}^2P^0_{3/2} - {}^2S^0_{1/2}$. Our results agree with [10] where GaAs (001) surface was irradiated by femtosecond (62 fs) focused titanium-sapphire radiation. Like our work, the processing was carried out in the air atmosphere. Experimental conditions with UV radiation focusing into the spot of 1 micron are extremely severe, they are far from conditions necessary for laser generation of point defects. As we hope, future sensitivity improvement of this experiment will be useful in analysis of the cloud over the sample surface at the condition of minimal sample damage.

3. SA with nano-structured barriers for 1040 nm

Our previous experience [3, 11, 12] in design and manufacturing of A_3B_5 semiconductor compounds based saturable absorbers was limited by multi-layer structures including quantum wells with thick barriers. In these cases quantum wells could be considered as isolated parts, and the number of quantum wells allowed to match a necessary level of saturable absorption. Experimental testing of one of our SA was realized in [3] for the home-made $Nd^{3+}:KGd(WO_4)_2$ laser operating at the wavelength of 1067 nm and pumped by diode laser at wavelength of 812 nm. In this case a stable passive mode-locking was achieved at the repetition rate of 70.5 MHz; the duration of individual pulses was estimated as 600 fs. Characterization of SA used in [3] by femtosecond pump-probe gave the "slow" relaxation time of about 188 ps.

The recovery time of SA is very important for obtaining spectral limited ultra-short pulses. The problem of the recovery time shortening is well known for all users and manufacturers of SA. The solutions for shortening of saturable absorber recovery time known in literature are numerous, they were partially cited in the Introduction.

Here we use another approach based on the idea of the coupled quantum wells [13, 14]. The fast tunneling of charge carriers between quantum wells should accelerate the recovery of linear absorption, avoid problems related to critical thickness of semiconductor layers in a presence of mechanical stress, and maintain good crystal quality. As a consequence, a high exciton contribution to the absorption can be expected.

Saturable absorber including multiple quantum wells of InGaAs separated by nano-structured barriers of GaAs was grown by molecular beam epitaxy (MBE) under permanent control of layers crystal quality by using high energy electrons diffraction. Results of the pump-probe testing of this sample are shown in the Fig. 6. Method of pump-probe measurements was described in detail in [3, 8]. The set up is based on femtosecond $Yb^{3+}:KY(WO_4)_2$ laser radiation of 200 fs duration; the beam was divided into two parts forming an exciting beam and a probe beam (at least 50 times lower in intensity and with orthogonal linear polarization). Both pump and probe beams were focused onto the sample surface into the spot of about 10 μm . The lock-in amplifier detected a signal representing the changes in the probe beam reflectivity of a sample induced by the pumping modulated at 880 Hz frequency. Time resolution of the measurements was determined by minimal step of optical delay line variation and was about 4 fs.

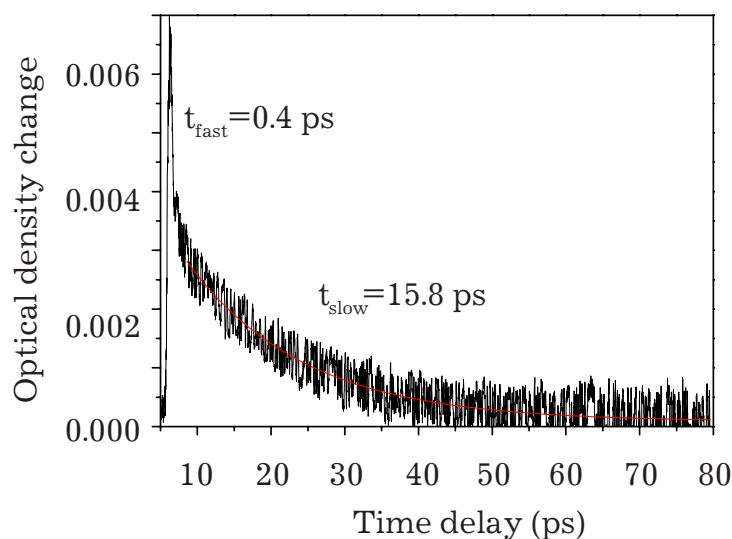


Figure 6. Fast (0.4 ps) and slow (15.8 ps) recovery of SA with nano-structured barriers.

The relative change of optical density of the sample is shown in Fig. 6 versus time delay

between pump and probe pulses. As usually, recovery kinetics contains two parts. The fast kinetics attributed to the ionization of excitons localized in quantum wells shows recovery time of about 0.4 ps. The slow part is related to charge carriers recombination with relaxation time of 15.8 ps. The presence of the fast part in recovery kinetics is a good sign, which confirms that exciton contribution to the absorption still exists. Slow relaxation proved an order of magnitude faster than in our previous SA with isolated quantum wells [3].

SA designed and manufactured by MBE growth on a base of this saturable absorber included conventional wide band total reflector and necessary number of quantum wells separated by nano-structured barriers. Linear spectrum of this SA showed reflectivity not less than 0.96 in the operation area of the $\text{Yb}^{3+}:\text{KY}(\text{WO}_4)_2$ laser of 1040 nm.

All the details for this SA (with nano-structured barriers) testing in $\text{Yb}^{3+}:\text{KY}(\text{WO}_4)_2$ laser can be found in [15]. Here, we describe briefly main results of [15]. The output power of $\text{Yb}^{3+}:\text{KY}(\text{WO}_4)_2$ laser in CW regime reached 1.62 W at the wavelength of 1043 nm for optical pumping power of 5.87 W. So, the optical pumping laser efficiency was 27.6%. The stable mode-locking regime was obtained in the same laser cavity after replacement of total reflector by the SA. The beam spot at the surface of SA was about 165 μm in diameter. The estimate for the saturating energy surface density is 120 $\mu\text{J}/\text{cm}^2$.

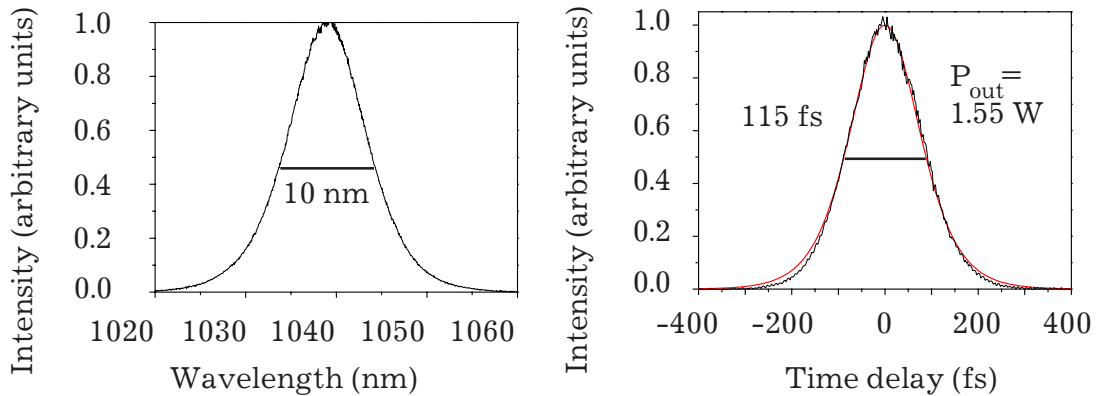


Figure 7. $\text{Yb}^{3+}:\text{KY}(\text{WO}_4)_2$ laser spectrum for the mode-locking regime induced by the fast SA (left graph) and autocorrelation function (noisy curve) with superimposed fitting curve (right graph).

Left part of Fig. 7 shows the $\text{Yb}^{3+}:\text{KY}(\text{WO}_4)_2$ laser spectrum for the mode-locking regime induced by the fast SA. The width at the half maximum is 10 nm, and the spectrum is centered at the wavelength of 1039 nm. Autocorrelation function in the right part of Fig. 7 is represented by the noisy curve. The model curve superimposed onto auto-correlation function is calculated as sech^2 , and it describes fine the experimental results. Ultra-short pulses duration of 115 fs should be attributed to the application of above described fast SA. Comparison of experimental spectral width and pulse duration gives the time-bandwidth product of 0.319. This means that the pulses are very close to the spectral limited type. The ultra-short pulses repetition rate was 70 MHz, and the peak power reached 171 kW. The maximum average power in the mode-locking regime was 1.57W. This value is very close to above mentioned value of 1.62 W in CW regime. Comparison of these two average power values confirms the low level of non-saturable losses introduced by fast SA.

4. Fast SA for 1500 nm region: preliminary results

Erbium laser operating in the vicinity of 1500 nm is another important laser source for the fast SA applications. We designed SA including thin quantum well layers of $\text{In}_{0.5}\text{Ga}_{0.5}\text{As}$ separated

by nano-structured barriers. The transmission spectra of SA is indicated in Fig. 8 for two samples. The lower curve represents SA transmission at GaAs substrate of $400\ \mu\text{m}$ thickness. The upper curve shows transmission for SA with partially removed substrate (mechanically to the thickness of about $10\ \mu\text{m}$). Both curves demonstrate the wide absorptive deep from 1080 to 1750 nm.

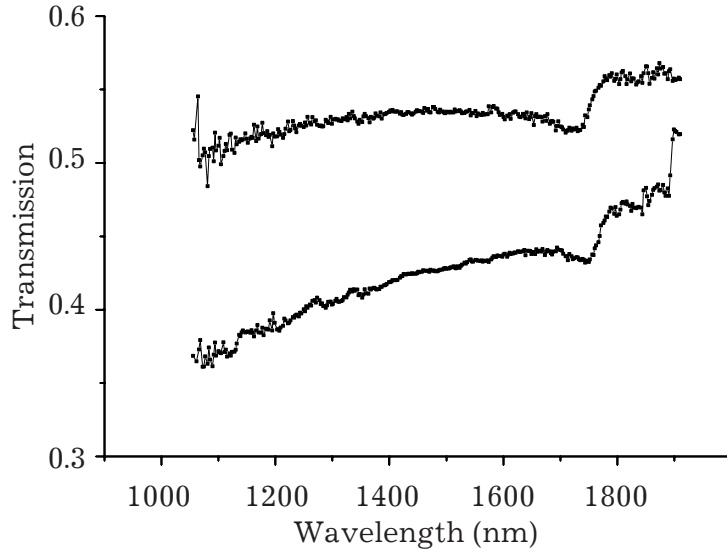


Figure 8. Transmission spectra for SA with nano-structured barriers. SA at GaAs substrate of $400\ \mu\text{m}$ (lower curve) and SA with partially removed substrate to the thickness $10\ \mu\text{m}$ (upper curve).

Reflectivity kinetics was tested at the wavelength of 1514 nm; the pump femtosecond pulse was generated by titanium-sapphire laser at the wavelength of 795 nm. Result is shown in left graph of Fig. 9 and clearly demonstrates very fast relaxation time.

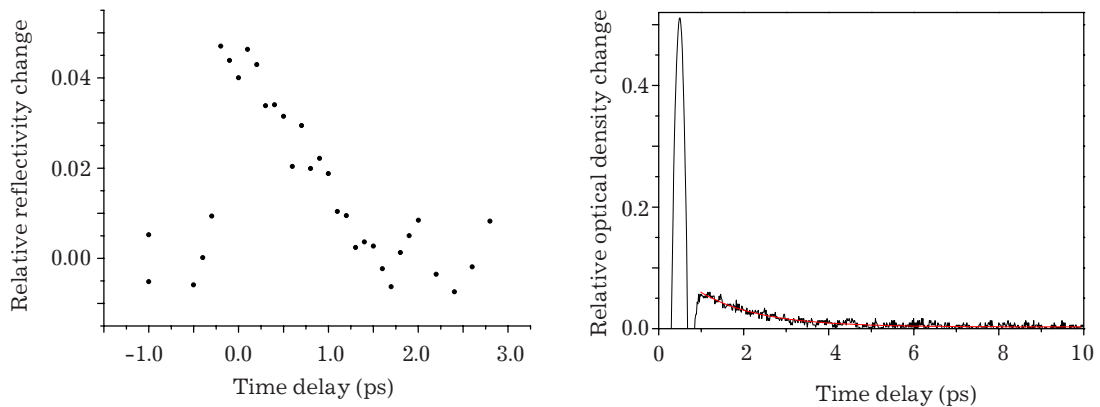


Figure 9. Reflectivity kinetics of fast SA at probe wavelength of 1514 nm (left graph) and at probe wavelength of 1040 nm (right graph).

SA reflectivity kinetics was checked also in another pump-probe set up based on femtosecond $\text{Yb}^{3+}:\text{KY}(\text{WO}_4)_2$ laser operating with 160 fs pulses at wavelength of 1040 nm. The probe beam at the same wavelength was two orders of magnitude lower than the pump one. The excitation

intensity in the SA was about 0.5 GW/cm^2 . Result is shown in the right graph of Fig. 9. The relaxation time for this kinetic curve equals to 1.3 ps.

So, SA with nanostructured barriers designed for the spectral area of 1500 nm demonstrated short relaxation times in both pump-probe experiments.

5. Discussion and summary

SA incorporating 20 quantum wells of GaAs separated by $\text{Al}_{0.38}\text{Ga}_{0.62}\text{As}$ barriers was irradiated by different number of UV laser pulses with different energy density. It was found experimentally, that PL intensity of SA sample decreases, and the electron-hole recombination rate increases with UV energy density. This effect revealed threshold nature with the threshold value of UV energy density of about 100 mJ/cm^2 — in agreement with [9]. Reflectivity kinetics of the SA sample detected at the probe radiation wavelength corresponding to the PL band maximum showed an increase of electron-hole recombination rate with growth of UV energy density — like in our experience with SA operating in the near-infrared region [8]. At the sharp focusing of UV laser radiation a laser plume formation over the sample surface was observed. The spectrum of the plume contained neutral gallium atoms doublet at wavelengths of 403 nm and 417 nm. This fact partially confirms the mechanism of point defects generation as a result of photo-chemical damage of the surface.

It is worth to stress that no visible damage of SA is observed if UV energy density lies under the threshold. Meanwhile, remarkable SA recovery time shortening was detected. So, UV treatment of semiconductor structures seems to be promising for their optical properties modification.

Another interesting point is the problem of point defects diffusion into the depth of the sample. In this work and in our previous work [8] we operated with SA including absorbing saturable layers placed near the surface. As is known, the penetration depth is extremely low for UV radiation. In the case of our experiments, the depth estimation gives the value of 13 nm (for GaAs at 308 nm UV wavelength) while the thickness of 20 quantum wells layer is about 180 nm. The penetration depth for laser radiation of 750 nm (or 780 nm) exciting photoluminescence (or pumping SA for reflectivity kinetics measurement) of the SA equals to hundreds of nanometers, and this means that PL signal (reflectivity signal) is generated by the whole set of 20 quantum wells. From this viewpoint, it would be interesting to compare results of UV irradiation by nanosecond pulses with the post-growth treatment of semiconductor structures by femtosecond pulses of UV radiation which should provide non-thermal mechanism of the surface damage like ablation.

It is well known, that SA should satisfy a series of very rigid requirements. First of all, it should provide necessary (for a given laser) level of saturable losses. Besides, SA relaxation time should lie in the range of few tens of picoseconds. Another evident requirement met by good SA is low level of nonsaturable losses. Taking into account all above mentioned, it is not surprising what a definitive role plays a special design and manufacturing of SA. Our result is obtained for $\text{Yb}^{3+}:\text{KY}(\text{WO}_4)_2$ laser stable mode-locking at 70 MHz, at central wavelength of 1039 nm, pulse length of 115 fs, maximum average power 1.57 W by using special fast SA of the own design and manufacturing; the pulses are close to spectral-limited type. Comparative experiments with commercially available SA mirror (BATOP GmbH, Germany) with close characteristics (absorption of about 3% at 1040 nm, relaxation time of 1 ps, saturating energy density of 50 J/cm^2) was also performed. The shortest pulse duration was increased to 148 fs, and the maximum average output power was decreased down to 1.37 W at the same level of the incident pump power. This also confirms that our SA mirror has lower level of non-saturable losses compared with other similar devices.

In conclusion, two techniques for the recovery time shortening of saturable absorbers on a base of A_3B_5 compounds including quantum wells were tested. The first one, proposed by authors,

is based on the post-growth treatment by UV laser radiation; it implied the generation of point defects, which, in its turn, led to the acceleration of electron-hole recombination and recovery time shortening by an order of magnitude and more. Another technique based on special design of barriers gave also promising results for the fast saturable absorbers. The semiconductor mirrors designed for the mode locking of infrared laser $\text{Yb}^{3+}:\text{KY}(\text{WO}_4)_2$ led to 115 fs stable mode-locking with average power close to CW regime. Preliminary results on fast saturable absorbers for spectral region of 1500 nm are also presented.

6. Acknowledgments

This research was supported by the Russian Foundation for Basic Research (grant 12-02-00327), by Presidium of the Russian Academy of Sciences Programme "Quantum mesoscopic and disordered structures" (grant 20.2), by by Presidium of the Russian Academy of Sciences Programme "Fundamental base of nano-structures and nano-materials technologies" (grant 24.20), and by Program of common fundamental research of Belarus National Academy of Science and Siberian Branch of Russian Academy of Science (grant No 14).

References

- [1] Pekarek S, Fiebig Ch, Stumpf M Ch, Oehler A E H, Paschke K, Erbert G, Südmeyer T, and Keller U 2010 *Optics Express* **18** 16320
- [2] Rubtsova N N, Kochubei S A, Kovalyov A A, Preobrazhenskii V V, Putyato M A, Pchelyakov O P, Semyagin B R, Shamirzaev T S, Kuleshov N V, Kisel V E, and Kurilchik S V 2010 *Proc. SPIE* **7721** 77210G
- [3] [Rubtsova N N, Kuleshov N V, Kisel' V E, Kovalyov A A, Kurilchik S V, Preobrazhenskii V V, Putyato M A, Pchelyakov O P, Shamirzaev T S 2009 *Laser Physics* **19** 285](#)
- [4] Tsuyoshi Okuno, Yasuaki Masumoto 2001 *Appl. Phys. Lett.* **79** 764
- [5] Du M Le, Harmand J C, Mauguin O, Largeau L, Travers L, Oudar J L 2006 *Appl. Phys. Lett.* **88** 201110
- [6] Soumalainen S, Vainionpää A, Tengvall O, Hakulinen T, Karirinne S, Guina M, Okhotnikov O G 2005 *Appl. Phys. Lett.* **87** 121106
- [7] Mangeney J, Oudar J L, Harmand J C, Meriafec C, Patriarche G, Aubin G, Stelmakh N, Lourtioz J M 2000 *Appl. Phys. Lett.* **76** 1371
- [8] [Rubtsova N N, Kuleshov N V, Kisel' V E, Kochubei S A, Kovalyov A A, Kurilchik S V, Preobrazhenskii V V, Putyato M A, Pchelyakov O P, Shamirzaev T S 2010 *Laser Physics* **20** 1262](#)
- [9] Kashkarov P K, Timoshenko V Yu 1995 *Poverkhnosyt'. Fizika, khimiya, mekhanika* **No 6** 5
- [10] Hu Zh, Singha S, Rich D H, and Gordon R G 2012 *Appl. Phys. Lett.* **100** 141102
- [11] [Kovalyov A A, Pchelyakov O P, Preobrazhenskii V V, Putyato M A, and Rubtsova N N 2007 *Laser Physics* **17** 478](#)
- [12] Kovalyov A A, Pchelyakov O P, Preobrazhenskii V V, Putyato M A, Rubtsova N N, Sorokin E, and Sorokina I T 2007 *Int. J. Nanosci.* **6** 315
- [13] Tackeuchi A, Muto S, Inata T, and Fujii T 1989 *Jpn. J. Appl. Phys.* **28** L1098
- [14] [Deveaud B, Chomette A, Clerot F, Auvray P, Regreny A, Ferreira R, and Bastard G 1990 *Superlattices Microstruct.* **8** 73](#)
- [15] [Kovalyov A A, Preobrazhenskii V V, Putyato M A, Pchelyakov O P, Rubtsova N N, Semyagin B R, Kisel' V E, Kuril'chik S V, Kuleshov N V 2011 *Laser Phys. Lett.* **8** 431](#)